Made available by Hasselt University Library in https://documentserver.uhasselt.be

Low bandgap polymers based on bay-annulated indigo for organic photovoltaics: Enhanced sustainability in material design and solar cell fabrication

Peer-reviewed author version

BREBELS, Jeroen; Klider, Karine C. C. W. S.; KELCHTERMANS, Mathias; VERSTAPPEN, Pieter; VAN LANDEGHEM, Melissa; VAN DOORSLAER, Sabine; Goovaerts, Etienne; Garcia, Jarem R.; MANCA, Jean; LUTSEN, Laurence; VANDERZANDE, Dirk & MAES, Wouter (2017) Low bandgap polymers based on bay-annulated indigo for organic photovoltaics: Enhanced sustainability in material design and solar cell fabrication. In: ORGANIC ELECTRONICS, 50, p. 264-272.

DOI: 10.1016/j.orgel.2017.07.037
Handle: http://hdl.handle.net/1942/25060

Low Bandgap Polymers Based on Bay-Annulated Indigo for Organic Photovoltaics: Enhanced Sustainability in Material Design and Solar Cell Fabrication

Jeroen Brebels,[a] Karine C. C. W. S. Klider,[a,b] Mathias Kelchtermans,[a] Pieter Verstappen,[a] Melissa Van Landeghem,[c] Sabine Van Doorslaer,[c] Etienne Goovaerts,[c] Jarem R. Garcia,[b] Jean Manca,[d] Laurence Lutsen,[e] Dirk Vanderzande,[a,e] and Wouter Maes[a,e]*

(a) UHasselt – Hasselt University, Institute for Materials Research (IMO-IMOMEC), Design & Synthesis of Organic Semiconductors (DSOS), Agoralaan, 3590 Diepenbeek, Belgium

(b) State University of Ponta Grossa (UEPG), Chemistry Department, Av. Gal. Carlos Cavalcanti, 4748, 84030-900 Ponta Grossa-PR, Brazil

(c) University of Antwerp, Physics Department, Universiteitsplein 1, 2610 Antwerpen, Belgium

(d) UHasselt – Hasselt University, X-LAB, Agoralaan, 3590 Diepenbeek, Belgium

(e) IMEC, Associated lab IMOMEC, Wetenschapspark 1, 3590 Diepenbeek, Belgium

Corresponding author: Tel.: +32 11268312; E-mail: wouter.maes@uhasselt.be

Abstract

Although research in the field of organic photovoltaics (OPV) still merely focuses on efficiency, efforts to increase the sustainability of the production process and the materials encompassing the device stack are of equally crucial importance to fulfil the promises of a truly renewable source of energy. In this study, a number of steps in this direction are taken. The photoactive polymers all contain an electron-deficient building block inspired on the natural indigo dye, bay-annulated indigo, combined with electron-rich thiophene and 4*H*-dithieno[3,2-*b*:2',3'-*d*]pyrrole units. The synthetic protocol (starting from indigo) is optimized and the final materials are thoroughly analyzed. MALDI-TOF mass spectrometry provides detailed information on the structural composition of the polymers. Best solar cell efficiencies are obtained for polymer:fullerene blends spin-coated from a pristine non-halogenated solvent (*o*-xylene), which is highly recommended to reduce the ecological footprint of OPV and is imperative for large scale production and commercialization.

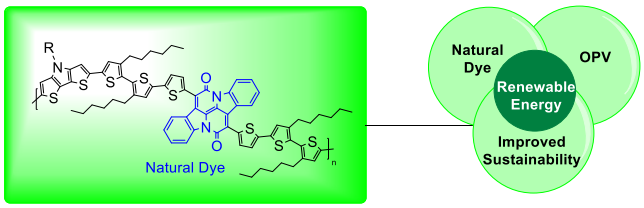

Key words

Bay-annulated indigo, Conjugated polymers, Nature-inspired dye, Organic photovoltaics, Renewable energy, Sustainability.

Introduction

Low bandgap conjugated (co)polymers consisting of alternating electron-rich (donor or 'push') and electron-poor (acceptor or 'pull') moieties in the polymer backbone have attracted a lot of attention during the last decade because of their interesting properties for organic electronics, in particular field-effect transistors (OFETs)[1,2] and photovoltaics (OPVs).[3] Because of the high absorptivity and suitability for printing of these types of organic semiconductors, fully flexible, ultra-thin photovoltaic devices can be produced. Other interesting properties such as semi-transparency and a better performance in diffuse light render OPV especially attractive for portable electronics and textile or building integration.[4-11] To absorb a maximum amount of solar light – from the UV throughout the visible up to the near-infrared (NIR) range – to be converted into electricity, the energy levels of the polymer absorbers must be fine-tuned on a molecular level.[12,13] This implies variation of the molecular structure to optimize the frontier orbital energy levels (HOMO and LUMO) and the resulting (low) bandgap. Simultaneously, appropriate solubility and miscibility with the electron-acceptor material is needed to achieve a near-ideal nanostructured bulk heterojunction (BHJ) active layer and a blend morphology maximizing charge extraction.[14]

A key step in improving OPV device efficiency is the quest for highly efficient donor and acceptor units creating photoactive push-pull type low bandgap copolymers or analogous small molecules. Recently, a novel acceptor chromophore based on the natural indigo dye, bay-annulated indigo (BAI), was reported as a promising building block for organic semiconducting materials.[15-20] The optical, electrochemical and charge carrier (hole/electron) mobility characteristics of the resulting low bandgap compounds are attractive for both electron donor and acceptor type OPV materials.[20] BAI shows several similarities with other lactam-based building blocks[21-24] affording highly efficient OPV materials (e.g. isoindigo[21] and diketopyrrolopyrrole or DPP; Figure 1). It is a strongly electron-deficient moiety because of the presence of two lactam units, resulting in a low-lying LUMO level, thereby rendering it an attractive acceptor unit for push-pull type low bandgap copolymers.[25] Furthermore, when proceeding from indigo to BAI, an enlarged planar structure is created, which improves the π- π stacking tendency of the resulting materials and hence facilitates intermolecular charge transport. Moreover, the BAI unit could also be used as an attractive precursor to design non-fullerene acceptor[26] materials.

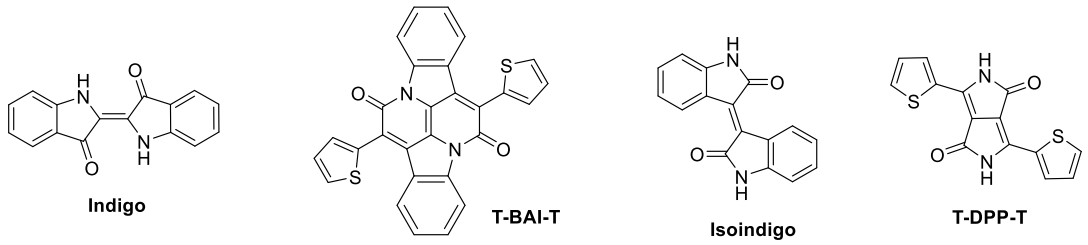

Figure 1. Lactam-based electron deficient building blocks.

Although recent achievements have pushed up the power conversion efficiencies (PCEs) of polymer solar cells to over 11% for single junction devices,[27] there is an eminent need for short, simple and scalable processes to reduce the synthesis costs of the active materials.[28-30] Furthermore, at present, the photoactive layers of the top-efficiency BHJ organic solar cells are most often produced from solutions in high-boiling chlorinated solvents with significant toxicity, such as (*ortho*-di)chlorobenzene.[26,31,32] These aromatic solvents are selected based on their solubilizing properties and the high boiling points lead to slow drying conditions, allowing for self-organization of the active components and the generation of favorable nanoscale blend morphologies. To reduce the ecological footprint of the OPV production process, especially upon upscaling, deposition from less harmful, non-halogenated solvents is highly desirable.[27,33-35] Recent studies have shown that *o*-xylene can be used as an alternative casting solvent, affording similar results as for chlorinated solvents.[36-42]

In the present study, *o*-xylene was found to be a superior processing solvent for active layer combinations of BAI-based copolymers and $PC_{71}BM$ ([6,6]-phenyl-C_{71}-butyric acid methyl ester). A device efficiency of 2.41% was achieved. Although the efficiency remains modest, this is among the highest values reported so far for OPV devices made from potentially bio-sustainable BAI-based materials.[15-20] The main importance of the reported results resides, however, in the reduced environmental impact of the active material development as well as the device processing. Moreover, MALDI-TOF mass spectrometry analysis of the final BAI-based polymers provided useful insights on the noticeably large variety of structures present in presumably simple alternating low bandgap copolymers.

Results and discussion

Material synthesis and characterization

Because of the increasing scarceness of crude oil, chemicals derived from non-fossil fuel resources are obviously gaining importance. In this respect, the natural dye indigo is highly attractive. Bay-annulated indigo (diindolonaphtyridine-6,13-dione) can be prepared from indigo in a single step. In this work, we have optimized the synthetic sequence toward thiophene-extended BAI derivative **2** (Scheme 1).[15] In the first step, a double annulation on indigo was performed with thiophene-2-acetyl chloride. Because of the (very) low solubility of precursor **1** and the formation of tar-like side products, more optimal reaction and purification conditions were pursued. *o*-Xylene was replaced by toluene as the reaction solvent, which resulted in less tar-like materials being formed, tentatively attributed to the lower boiling point of the applied solvent. After the reaction, it was found to be crucial to first purify the product by Soxhlet extractions with acetone and chloroform (recovering the material) before final recrystallization. This approach provides a more pure product (see ^{1}H NMR spectrum in the supporting information). No elaborate purification methods were required, in contrast to other literature procedures affording comparable yields.[19,20] In the next step, dibromination was performed with *N*-bromosuccinimide (NBS) in DMF, which reduced the solubility of the

BAI core even further. Bromination was performed at 60 °C to completely solubilize the starting material and hence obtain complete conversion without too much (over)heating.

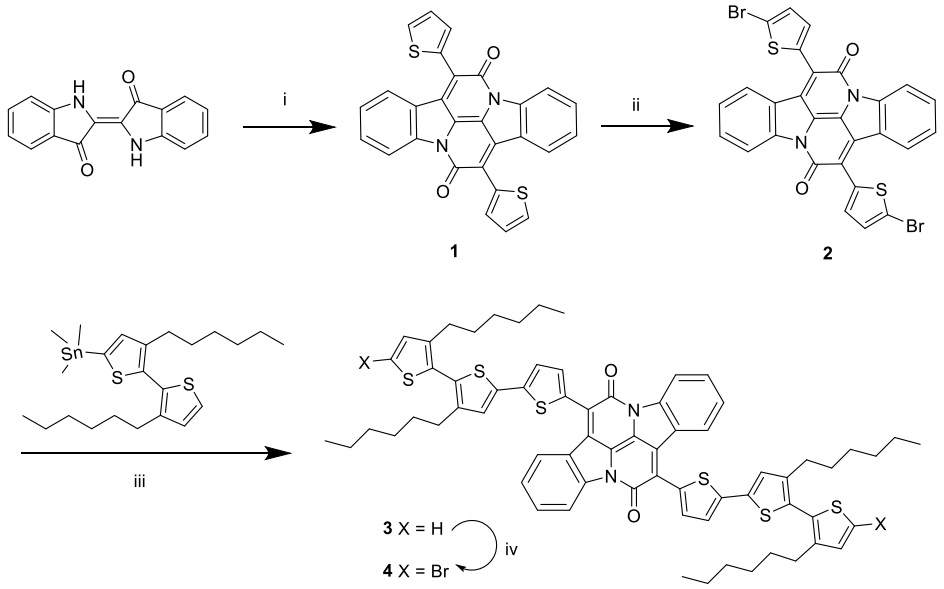

Scheme 1. BAI monomer synthesis: i) thiophene-2-acetyl chloride, toluene, reflux, 72 h (27%); ii) NBS, DMF, 60 °C, 3 h (84%); iii) $Pd(PPh_3)_4$, toluene, DMF, reflux, 16 h (55%); iv) NBS, $CHCl_3$, RT, 16 h (76%).

To increase the solubility of the BAI precursor, we decided to extend the chromophore with an alkylated bithiophene moiety (Scheme 1). To this extent, mono-stannylation of a hexylated 2,2'-bithiophene unit was performed first, and then this moiety was introduced on BAI compound **2** via a Stille cross-coupling reaction employing $Pd(PPh_3)_4$ as the catalyst. An analogous Suzuki protocol was tested as well, affording similar results and avoiding the formation of toxic tin residues. Product **3** was considerably more soluble and therefore it was easily purified by column chromatography. The moderate yield (55%) might be due to remaining impurities in the starting product **2**. In the final step, bromination with NBS in $CHCl_3$ was performed and the desired monomer **4** was readily obtained.

From this novel BAI monomer, a first polymer was prepared by combining it with 2,5-bis(trimethylstannyl)thiophene in a Stille cross-coupling polycondensation. However, an insoluble material was obtained, indicating that alkylated donor building blocks are required to render the final low bandgap polymers soluble and processable. Because of our previous successes with 4*H*-dithieno[3,2-*b*:2',3'-*d*]pyrrole (DTP) derivatives,[43-45] we turned to these electron-rich precursors. At first, the N-alkylated DTP unit **5a** was synthesized starting from 3,3'-dibromo-2,2'-bithiophene and 2-octyldodecan-1-amine (Scheme 2). Subsequently, distannylation with trimethyltin chloride was performed to obtain DTP monomer **6a**.[46] A relatively long branched side chain was introduced to overcome solubility problems in the resulting polymer. Two other DTP-*alt*-BAI polymers were synthesized as well. However, for these polymers, the N-alkyl substituent on the DTP part was replaced by an N-acyl unit, which has been shown before to lower the HOMO level of the resulting polymers and hence afford an increased open-circuit voltage (V_{oc}) in the final solar cells.[43-47] The required

bis(trimethylstannyl)-DTP monomers, 1-[2,6-bis(trimethylstannyl)-4*H*-dithieno[3,2-*b*:2',3'-*d*]pyrrol-4-yl]-2-hexyldecan-1-one (**9b**) and 1-[2,6-bis(trimethylstannyl)-4*H*-dithieno[3,2-*b*:2',3'-*d*]pyrrol-4-yl]-2-butyloctan-1-one (**9c**) (Scheme 2), were prepared according to literature procedures.[43,47] A copper-catalyzed reaction between 3,3'-dibromo-2,2'-bithiophene and the respective amide-functionalized side chain was performed, followed by dibromination with NBS and final distannylation with hexamethylditin (Scheme 2). All final monomers were purified by (recycling) preparative size exclusion chromatography (prep-SEC) to eliminate residual impurities, allowing a proper stoichiometric balance in the polymerization reactions. This is essential to achieve high molar masses, as generally required for efficient polymer solar cells.[48-51]

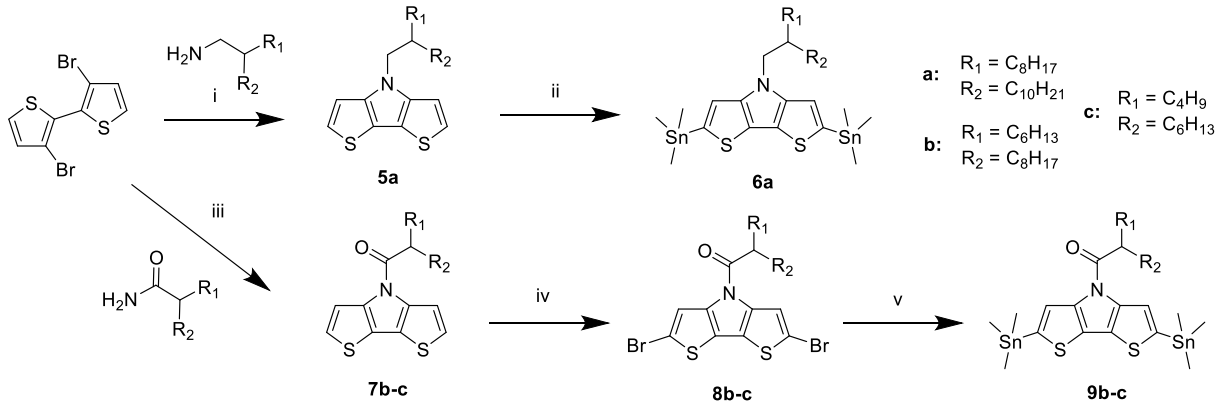

Scheme 2. DTP monomer synthesis: i) *t*BuONa, $Pd_2(dba)_3$, BINAP, toluene, reflux, 16 h (86%); ii) *n*-BuLi, $(CH_3)_3SnCl$, -78 °C, 5 h (58%); iii) K_2CO_3, CuI, DMEDA, toluene, reflux, 24 h (57%); iv) NBS, $CHCl_3$, 0 °C, 2 h (93%); v) $(CH_3)_3SnSn(CH_3)_3$, LiCl, $Pd(PPh_3)_4$, toluene, reflux, 1 h (59%).

The different monomers were then copolymerized using a Stille polycondensation approach under standard conditions (2 mol% Pd_2dba_3, 8 mol% P(*o*-tol)$_3$, toluene/DMF, reflux, 16 h; Scheme 3). After the reactions, the crude polymer materials were precipitated in methanol and further purified using Soxhlet extractions with different solvents (acetone, *n*-hexane and chloroform successively, for at least 2 hours) to remove catalyst residues and low molar mass species. Finally, polymers with number-averaged molar masses (M_n) of 29, 55 and 20 kg/mol for **P1**, **P2** and **P3**, respectively, were obtained (Table 1). The lower M_n observed for **P3** can be attributed to the fact that it already precipitated during the polymerization, prohibiting it to react any further. The final polymer material (**P3**) was only soluble in high boiling point solvents (e.g. hot chlorobenzene).

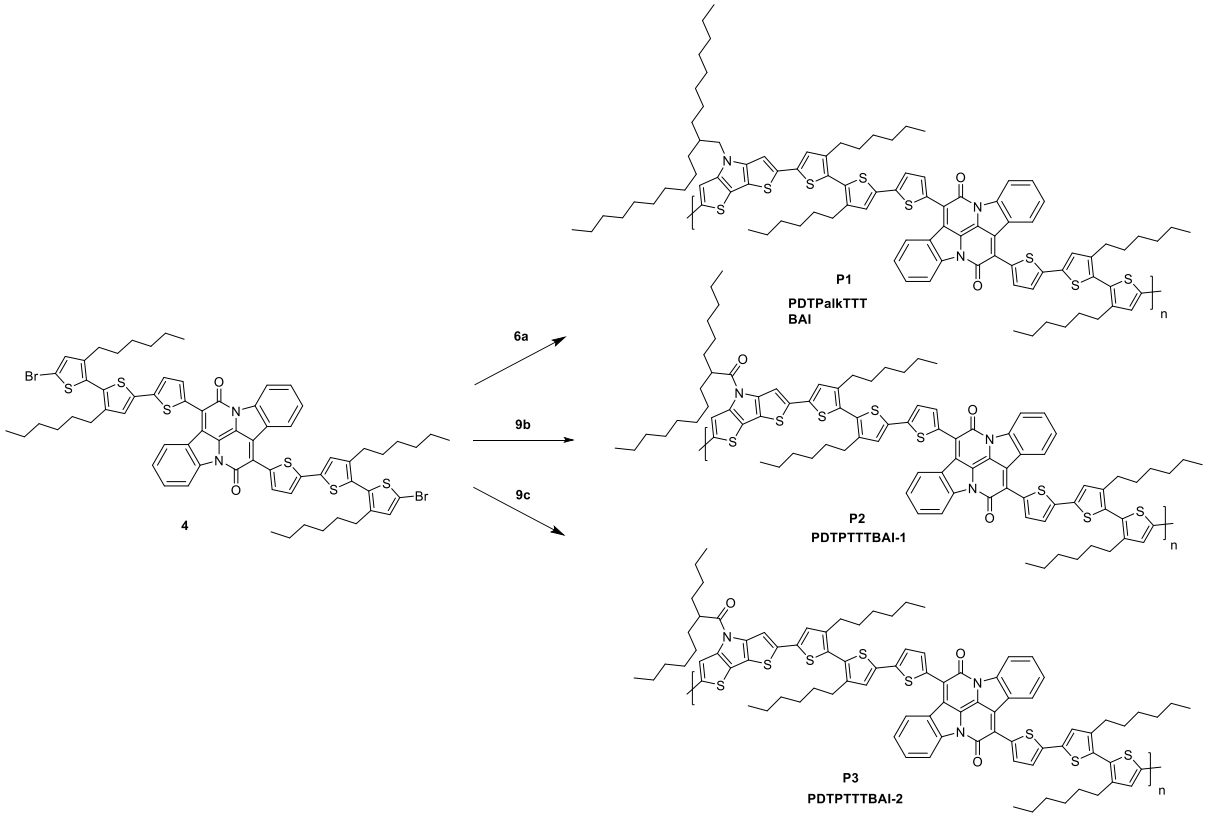

Scheme 3. BAI-*alt*-DTP polymer synthesis by Stille cross-coupling (similar reaction conditions for all polymerizations: 2 mol% Pd_2dba_3, 8 mol% P(*o*-tol)$_3$, toluene/DMF, reflux, 16 h).

MALDI-TOF (matrix-assisted laser desorption ionization time-of-flight) mass spectrometry was applied to gain more information on the exact nature of the products within the polymer distribution. Although such analysis is rarely performed for low bandgap copolymers, MALDI-TOF can provide important insights on the polymer composition that cannot trivially be obtained by other techniques. The MALDI-TOF spectra (Figure 2, 3 and S1-S4) are similar for the three polymers. Besides the expected alternating oligomer-like species, homocoupling of both the acceptor (BAI) and donor (DTP) monomers was observed as well, probably generating a stoichiometric imbalance during the polymerization and thereby hindering the formation of high molar masses. The strong impact of homocoupling 'defects' on the final solar cell performance has recently been elucidated in a number of studies.[45,50,52-54] As such, direct identification of homocoupling via MALDI-TOF is very relevant. Furthermore, MALDI-TOF also allows identifying the end groups of the different polymer chains. In this particular case, reactive bromide end groups were still observed for polymers **P1** and **P3**. Moreover, methyl end-capping is also seen regularly, pointing to methyl transfer from the trimethylstannyl precursors as an important polymer termination reaction.[55] The lower molar masses observed in the MALDI-TOF spectra as compared to the SEC data are a result of the overestimation of the molar masses derived from SEC (because of the polystyrene standards used and the tendency of the polymers to aggregate) and the use of lower molar mass fractions for the MALDI-TOF analysis (to facilitate the sample preparation, improve the signal to noise ratio and allow structural analysis).

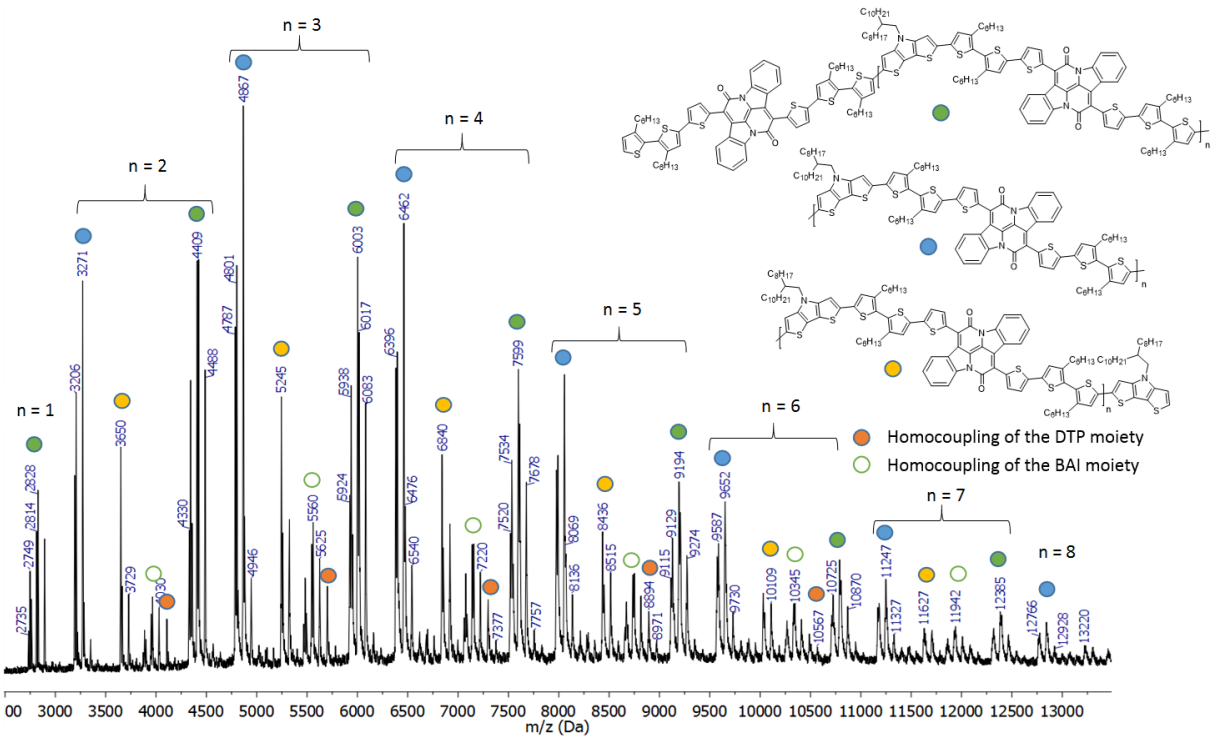

Figure 2. MALDI-TOF mass spectrum of **P1**.

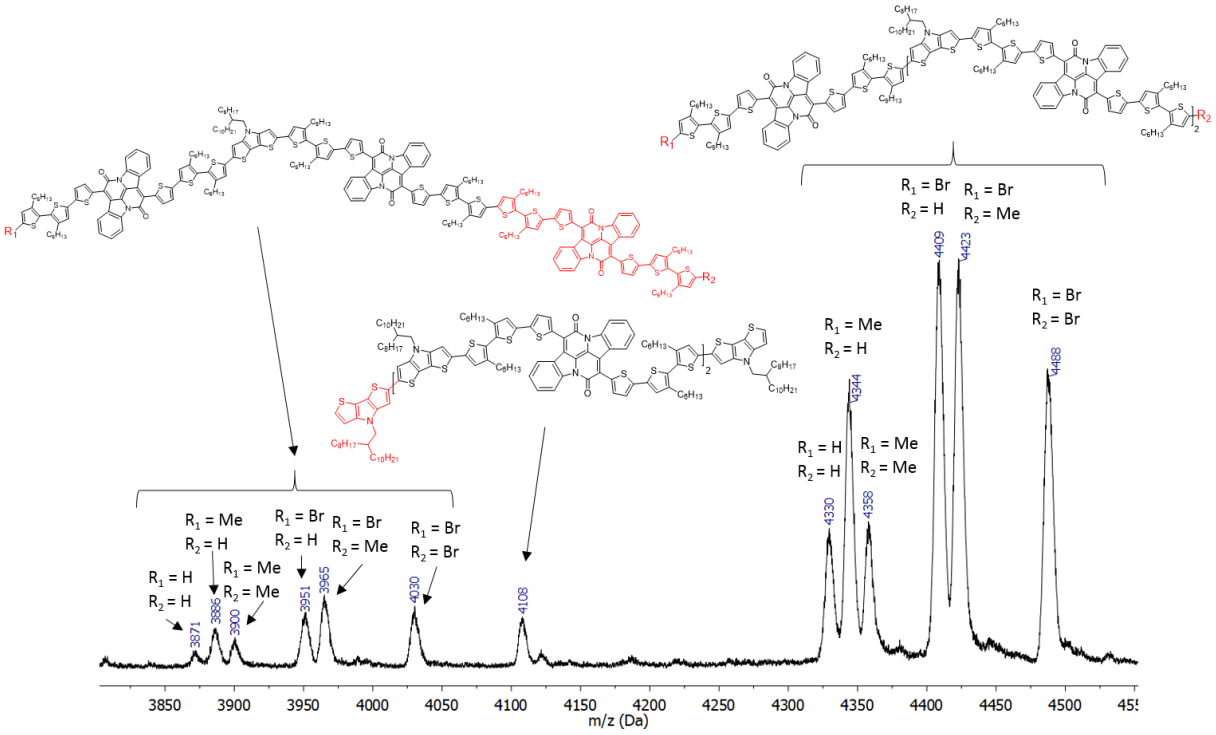

Figure 3. MALDI-TOF mass spectrum of **P1** (zoom from *m/z* 3800 to 4550 g mol^{-1}), with the assignment of homocoupling and end group identification.

The thermal properties of the polymers were investigated by thermogravimetric analysis (TGA) and rapid heat-cool calorimetry (RHC) (Figure S5-S7, Table 1). TGA showed that the polymers are thermally stable (i.e. they do not lose any mass) up to 300 °C. RHC was chosen above regular differential scanning calorimetry (DSC) because of its increased sensitivity to

thermal transitions resulting from the fast scanning rates and the low sample amounts required.[56] RHC analysis indicated that all polymers are fully amorphous in the second heating (after a preceding cooling at 20 K min^{-1}), whereas some endo/exothermic behavior between 70 and 150 °C was seen in the first heating (Figure S6, S7). A glass transition (T_g) between 130 and 150 °C was observed in the second heating for all three materials. These high T_g's are beneficial for the thermal stability of the bulk heterojunction blends.[57-60]

The optical and electrochemical properties of the three polymers were also investigated to analyze the suitability of the novel materials for polymer solar cells and to establish structure-property relations. Figure 4 shows the UV-Vis-NIR absorption spectra in chlorobenzene solution and in the solid state. All polymers exhibit a broad dual band absorption in the 350–900 nm region. A notable extension to the NIR is observed compared to standard low bandgap polymers because of the highly electron-deficient nature of the BAI moiety. Polymer **P1** shows the largest bathochromic shift, which can be attributed to the increased donor strength of the N-alkylated DTP component. In all cases, peak broadening is observed when going from solution to the solid state, pointing to π-π stacking and therefore strong electronic interactions in the films. The optical bandgaps, estimated from the absorption edges of the polymer films, are all similar and around 1.4 eV (Table 1). The absorption coefficients of the three polymers in chlorobenzene solution are in the range of 43–55 L g^{-1} cm^{-1} (Table 1, Figure S8). The differences can be due to the different DTP monomers employed (N-alkyl vs N-acyl), molar mass and/or side chain (volume fraction) variations.[61]

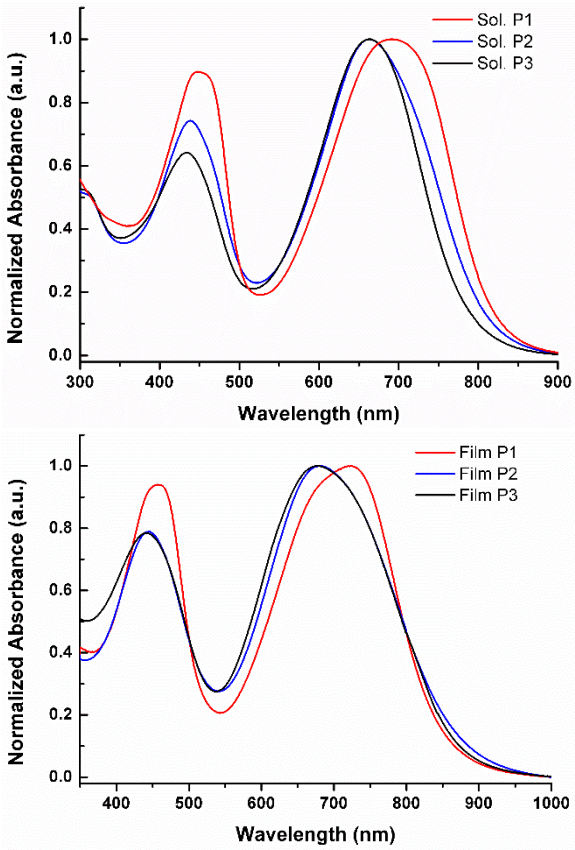

Figure 4. Normalized UV-Vis-NIR absorption spectra for **P1**, **P2** and **P3** in chlorobenzene solution (top) and thin film (bottom).

Table 1. Molar mass, optical, thermal and electrochemical data for copolymers **P1**, **P2** and **P3**.

	M_n[a]/ kg mol^{-1}	$Đ$	$\lambda_{max\ film}$[b]/ nm	ε[c] / L g^{-1} cm^{-1}	Eg_{film}[d]/ eV	T_g[e]/ °C	E_{ox}[f]/ eV	E_{red}[f]/ eV	Eg_{cv}[g]/ eV	E_{HOMO}[h]/ eV	E_{LUMO}[h]/ eV
P1	29	4.4	723	43.0	1.46	130	0.29	−1.11	1.40	−5.2(6)	−3.9
P2	55	3.3	680	54.9	1.41	134	0.34	−1.11	1.44	−5.3(0)	−3.9
P3	20	1.7	677	52.4	1.41	149	0.34	−1.16	1.50	−5.3(1)	−3.8

[a] Measured by SEC at 60 °C in chlorobenzene. [b] Films were prepared by drop-casting a solution of the polymer onto a quartz disc. [c] Extinction coefficient of the polymers in chlorobenzene solution at λ_{max}. [d] Optical bandgap, determined by the onset of the solid-state UV-Vis-NIR spectrum. [e] Glass transition temperature (2nd heating). [f] Onset potentials vs. Fc/Fc^+. [g] Electrochemical bandgap. [h] Determined from the onset of oxidation/reduction in cyclic voltammetry.

The electrochemical features of the polymers were investigated by cyclic voltammetry (CV; Figure S9, S10, Table 1). HOMO and LUMO energy levels were estimated from the oxidation and reduction onset potentials. As expected, a deeper HOMO level was observed when introducing the N-acyl substituent on the DTP part.[43,47] From the data obtained, there seems to be no (substantial) LUMO-LUMO offset with $PC_{71}BM$ (E_{red} = −1.26 eV under the same experimental CV conditions; Figure S9), suggesting that the polymers might not act as efficient electron donors in combination with $PC_{71}BM$. To investigate the charge-transfer mechanism between the polymers and $PC_{71}BM$, light-induced electron paramagnetic resonance (LI-EPR) experiments were performed on the **P2**:$PC_{71}BM$ (1:4) blend. The X-band (9.4 GHz) and W-band (94 GHz) LI-EPR spectra (Figure S11) enabled the identification of the positive and negative radicals formed in the blend after charge transfer, based on their respective electronic g-tensors. By comparison of the experimental g-values with those obtained from our density functional theory (DFT) calculations (Table S1, Figure S12, S13) and literature values for the $PC_{71}BM$ anion,[62] the EPR spectra could be unambiguously assigned to positive radicals on the **P2** polymer (with the deepest LUMO in the series) and negative radicals on the fullerene molecules, thereby confirming the donor character of the polymers relative to $PC_{71}BM$.

OPV device fabrication and analysis

The photovoltaic performances of the novel materials were then investigated by fabricating BHJ organic solar cells with a traditional device architecture consisting of glass/ITO/PEDOT:PSS/polymer:$PC_{71}BM$/Ca/Al. The device measurements were carried out under illumination of AM1.5G simulated solar light (100 mW cm^{-2}) and the photovoltaic properties are summarized in Table 2.

Polymer **P1** showed a good solubility in all common processing solvents. On the other hand, due to the low solubility of **P2** and **P3**, high-boiling aromatic solvents (e.g. chlorobenzene, *o*-

xylene, ...) were needed to completely dissolve these polymers and to process the active layers. The performance of the BHJ solar cells was first optimized by changing the polymer to $PC_{71}BM$ ratios and layer thicknesses of the blends. **P1** showed an optimal polymer:fullerene weight ratio of 1:3, whereas for **P2** and **P3**, 1:4 turned out to be the best ratio, with optimal layer thicknesses around 80−90 nm for all devices. At first, the devices made from **P1** were further optimized. Unfortunately, however, modest efficiencies (up to a PCE of 1.24%) were obtained in all cases. Especially the V_{oc} and fill factor (FF) turned out to be the limiting factors (Table 2, S2, Figure S15). Replacement of the alkyl substituents on the DTP units by acyl derivatives notably improved the V_{oc},[43,47] in accordance with the electrochemical data. Careful optimization of the processing solvent for the **P3**:$PC_{71}BM$ blends afforded a best performing device with a PCE of 1.84% from chlorobenzene (Table S4, Figure S16). Upon annealing at 85 °C for 10 minutes, the efficiency further improved to 2.22% (J_{sc} = 6.83 mA cm^{-2}, V_{oc} = 0.80 V, FF = 0.41; Table 2). Despite the higher M_n of **P2**, similar device results were initially achieved. However, as this polymer is also soluble in *o*-xylene, this processing solvent could also be applied. *o*-Xylene is a 'greener' alternative for the most commonly used halogenated processing solvents. It has a high boiling point and is a suitable candidate for high-throughput OPV production.[36-42] In our case, *o*-xylene turned out to be the best choice and a record PCE of 2.41% (J_{sc} = 6.67 mA cm^{-2}, V_{oc} = 0.82 V, FF = 0.44; Figure 5, Table 2) was achieved after annealing at 110 °C for 10 minutes. To further improve the efficiency, anisaldehyde was used as a co-solvent in various volume concentrations (1 to 2% v/v).[37] Unfortunately, however, the PCE did not increase any further (Table 2). The EQE spectrum shows a broad charge photogeneration (J_{EQE} = 6.82 mA cm^{-2}) range from 300 up to 900 nm, hence extending into the NIR (Figure S17). Expansion to the NIR is considered to be a main challenge for OPV and is important to further improve the efficiency of state-of-the-art devices.[20,52] Despite extensive optimization efforts, modest device efficiencies were still obtained, which can tentatively be attributed to the low/average molar masses obtained, the presence of homocoupling in all three polymer compositions and the modest driving force for electron transfer. Nevertheless, one of the highest PCE's for a BHJ solar cell made from a BAI-based polymer material was achieved.[15-20]

Table 2. Photovoltaic output parameters for the BHJ organic solar cells based on copolymers **P1**, **P2** and **P3** (in combination with $PC_{71}BM$).

Polymer	Solvent[a]	Ratio	Additive	V_{oc} / V	J_{sc} / mA cm^{-2}	FF	Best PCE[c] / %
P1	CF	1:3	/	0.64	5.37	0.36	1.24 (1.22)
P2	CB	1:4	10% TCE[b] (annealed @85 °C)	0.78	6.99	0.42	2.28 (2.25)
P2	*o*-xylene	1:4	/ (annealed @110 °C)	0.82	6.67	0.44	2.41 (2.28)
P2	*o*-xylene	1:4	1% anisaldehyde (annealed @110 °C)	0.80	6.47	0.45	2.31 (2.13)
P3	CB	1:4	/ (annealed @85 °C)	0.80	6.83	0.41	2.22 (2.06)

[a] CF = chloroform, CB = chlorobenzene. [b] TCE = tetrachloroethane. [c] Average efficiencies over at least 3 devices in brackets.

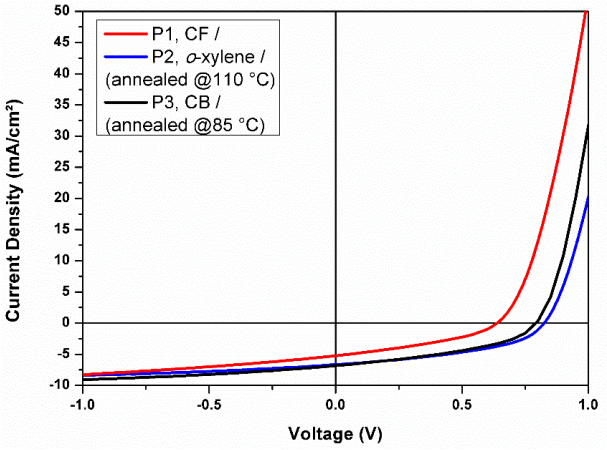

Figure 5. *J-V* characteristics of the best polymer solar cells prepared from the **P1**–**P3**:$PC_{71}BM$ blends.

The limited FF and J_{sc} values cannot simply be attributed to a too low hole mobility of the new donor polymers. The saturated hole mobilities for the **P1** and **P2** polymers as measured in OFETs were similar and in the appropriate range (1×10^{-3} cm²/Vs for **P1** and 3×10^{-3} cm²/Vs for **P2**). Most often, a less than optimal active layer morphology is at the origin of OPV blends performing below expectations. The surface morphology of the best performing active layer blend was investigated with atomic force microscopy (AFM) in tapping mode (Figure S18). A rather rough morphology was observed, with large particles remaining in the active layer, which is in agreement with the moderate FF values observed. These large domains also reduce the donor-acceptor interface and hence the dissociation of excitons into free charges, thereby limiting the J_{sc}. The addition of 1% (v/v) anisaldehyde as co-solvent did not improve the surface morphology, providing even larger domains (Figure S18), in accordance with the values of the OPV parameters.

Conclusions

Three push-pull type copolymers employing bay-annulated indigo as the electron deficient and 4*H*-dithieno[3,2-*b*:2',3'-*d*]pyrrole as the electron rich building block were synthesized, with particular attention for the synthetic protocol of the nature-inspired BAI monomer. MALDI-TOF mass spectrometry provided detailed information on the structural composition of the polymers, indicating homocoupling defects as well as methyl shift termination reactions. Photophysical and electrochemical analysis pointed out that the polymers possess relatively small bandgaps (~1.4 eV) and low-lying LUMO levels. Nevertheless, EPR analysis showed that the polymers act as electron donors in combination with $PC_{71}BM$. The polymers were then all tested in bulk heterojunction solar cells, affording a maximum efficiency of 2.41%, which is among the highest efficiencies reported so far for organic photovoltaics prepared from BAI-containing active materials. Photocurrent is generated throughout the complete visible spectrum up to the NIR range. Noteworthy, the optimal result was achieved

using a non-halogenated processing solvent (*o*-xylene), which is beneficial from an ecological point of view. As the device performance seems to be partly limited by the non-favorable active layer morphology, current efforts focus on the introduction of different donor building blocks to increase the miscibility of the final BAI-based polymers with suitable electron acceptors, in particular non-fullerene materials with low-lying LUMO levels. On the other hand, the NIR activity of the blends can also beneficially be applied in organic photodetectors.[63] Finally, further efforts are required toward a truly 'green' synthesis of BAI-based organic semiconductors.[64]

Acknowledgements

This work was supported by the Research Foundation – Flanders (FWO Vlaanderen) (projects G.0415.14N, G.0B67.15N and RADESOL, PhD fellowship M. Van Landeghem). J. Brebels and M. Kelchtermans acknowledge the Agency for Innovation by Science and Technology in Flanders (IWT) for their PhD grants. K.C.C.W.S. Klider acknowledges the Brazilian National Council for Scientific and Technological Development (CNPq) for her Sandwich PhD scholarship. The authors are grateful to B. Van Mele and M. Defour for the thermal analysis, and H. Penxten for the CV measurements.

Supporting information

Experimental data, ^{1}H and ^{13}C NMR spectra, MALDI-TOF mass spectra and structure assignment of **P2** and **P3**, thermal analysis, oxidation and reduction curves (CV), EPR data, solar cell optimization data, the EQE spectrum of the optimized device prepared from **P2** and AFM images can be found in the Supporting Information.

References

[1] Kim, G.; Kang, S.-J.; Dutta, G. K.; Han, Y.-K.; Shin, T. J.; Noh, Y.-Y.; Yang, C. A Thienoisoindigo-Naphthalene Polymer with Ultrahigh Mobility of 14.4 cm^2/V·s that Substantially Exceeds Benchmark Values for Amorphous Silicon Semiconductors. *J. Am. Chem. Soc.* **2014**, *136* (26), 9477-9483.
[2] Yamashita, Y.; Hinkel, F.; Marszalek, T.; Zajaczkowski, W.; Pisula, W.; Baumgarten, M.; Matsui, H.; Müllen, K.; Takeya, J. Mobility Exceeding 10 cm^2/(V·s) in Donor-Acceptor Polymer Transistors with Band-like Charge Transport. *Chem. Mater.* **2016**, *28* (2), 420-424.
[3] Müllen, K.; Pisula, W. Donor-Acceptor Polymers. *J. Am. Chem. Soc*. **2015**, *137* (30), 9503-9505.
[4] Dennler, G.; Scharber, M. C.; Brabec, C. J. Polymer-Fullerene Bulk-Heterojunction Solar Cells. *Adv. Mater.* **2009**, *21* (13), 1323-1338.
[5] Kaltenbrunner, M.; White, M. S.; Głowacki, E. D.; Sekitani, T.; Someya, T.; Sariciftci, N. S.; Bauer, S. Ultrathin and lightweight organic solar cells with high flexibility. *Nat. Commun.* **2012**, *3*, 770.

[6] Su, Y. W.; Lan, S. C.; Wei, K. H. Organic Photovoltaics. *Mater. Today* **2012**, *15* (12), 554-562.
[7] Darling, S. B.; You, F. The case for organic photovoltaics. *RSC Adv.* **2013**, *3*, 17633-17648.
[8] Lizin, S.; Van Passel, S.; De Schepper, E.; Maes, W.; Lutsen, L.; Manca, J.; Vanderzande, D. Life cycle analyses of organic photovoltaics: a review. *Energy Environ. Sci.* **2013**, *6*, 3136-3149.
[9] Dou, L.; You, J.; Hong, Z.; Xu, Z.; Li, G.; Street, R. A.; Yang, Y. 25th Anniversary Article: A Decade of Organic/Polymeric Photovoltaic Research. *Adv. Mater.* **2013**, *25* (46), 6642-6671.
[10] Mazzio, K. A.; Luscombe, C. K. The future of organic photovoltaics. *Chem. Soc. Rev.* **2015**, *44*, 78-90.
[11] Kang, H.; Kim, G.; Kim, J.; Kwon, S.; Kim, H.; Lee, K. Bulk-Heterojunction Organic Solar Cells: Five Core Technologies for Their Commercialization. *Adv. Mater.* **2016**, *28* (36), 7821-7861.
[12] Havinga, E. E.; Ten Hoeve, W.; Wynberg, H. A new class of small band gap organic polymer conductors. *Polym. Bull.* **1992**, *29* (1), 119-126.
[13] Kitamura, C.; Tanaka, S.; Yamashita, Y. Design of Narrow-Bandgap Polymers. Syntheses and Properties of Monomers and Polymers Containing Aromatic-Donor and o-Quinoid-Acceptor Units. *Chem. Mater.* **1996**, *8* (2), 570-578.
[14] Park, S. H.; Roy, A.; Beaupré, S.; Cho, S.; Coates, N.; Moon, J. S.; Moses, D.; Leclerc, M.; Lee, K.; Heeger, A. J. Bulk heterojunction solar cells with internal quantum efficiency approaching 100%. *Nature Photon.* **2009**, *3*, 297-303.
[15] He, B.; Pun, A. B.; Zherebetskyy, D.; Liu, Y.; Liu, F.; Klivansky, L.; McGough, A. M.; Zhang, B. A.; Lo, K.; Russell, T. P.; Wang, L.; Liu, Y. New Form of an Old Natural Dye: Bay-Annulated Indigo (BAI) as an Excellent Electron Accepting Unit for High Performance Organic Semiconductors. *J. Am. Chem. Soc.* **2014**, *136* (42), 15093-15101.
[16] He, B.; Zherebetskyy, D.; Wang, H.; Kolaczkowski, M.; Klivansky, L. M.; Tan, T.; Wang, L.; Liu, Y. Rational Tuning of the High Energy Visible Light Absorption for Panchromatic Small Molecules by a Two-Dimensional Conjugation Approach. *Chem. Sci.* **2016**, *7*, 3857-3861.
[17] He, B.; Neo, W. T.; Chen, T. L.; Klivansky, L. M.; Wang, H.; Tan, T.; Teat, S. J.; Xu, J.; Liu, Y. Low Bandgap Conjugated Polymers Based on a Nature-Inspired Bay-Annulated Indigo (BAI) Acceptor as Stable Electrochromic Materials. *ACS Sustainable Chem. Eng.* **2016**, *4* (5), 2797-2805.
[18] Kolaczkowski, M.; He, B.; Liu, Y. Stepwise Bay Annulation of Indigo for the Synthesis of Desymmetrized Electron Acceptors and Donor−Acceptor Constructs. *Org. Lett.* **2016**, *18* (20), 5224-5227.
[19] Fallon, K. J.; Wijeyasinghe, N.; Manley E. F.; Dimitrov, S. D.; Yousaf, S. A.; Ashraf, R. S.; Duffy, W.; Guilbert, A. A. Y.; Freeman, D. M. E.; Al-Hashimi, M.; Nelson, J.; Durrant, J. R.; Chen, L. X.; McCulloch, I.; Marks, T. J.; Clarke, T. M.; Anthopoulos, T. D.; Bronstein, H. Indolo-naphthyridine-6,13-dione Thiophene Building Block for Conjugated Polymer Electronics: Molecular Origin of Ultrahigh n-Type Mobility. *Chem. Mater.* **2016**, *28* (22), 8366-8378.
[20] Fallon, K. J.; Wijeyasinghe, N.; Yaacobi-Gross, N.; Ashraf, R. S.; Freeman, D. M. E.; Palgrave, R. G.; Al-Hashimi, M.; Marks, T. J.; McCulloch, I.; Anthopoulos, T. D.; Bronstein, H. A Nature-Inspired Conjugated Polymer for High Performance Transistors and Solar Cells. *Macromolecules* **2015**, *48* (15), 5148-5154.
[21] Wang, E.; Mammo, W.; Andersson, M. R. 25th Anniversary Article: Isoindigo-Based Polymers and Small Molecules for Bulk Heterojunction Solar Cells and Field Effect Transistors. *Adv. Mater.* **2014**, *26* (12), 1801-1826.
[22] Cao, J.; Liao, Q.; Du, X.; Chen, J.; Xiao, Z.; Zuo, Q.; Ding, L. A pentacyclic aromatic lactam building block for efficient polymer solar cells. *Energy Environ. Sci.* **2013**, *6*, 3224-3228.

[23] Qian, L.; Cao, J.; Ding, L. A hexacyclic ladder-type building block for high-performance D-A copolymers. *J. Mater. Chem. A* **2015**, *3*, 24211-24214.
[24] Cao, J.; Qian, L.; Ding, L. A heptacyclic acceptor unit developed for D-A copolymers used in polymer solar cells. *Polym. Chem.* **2016**, *7*, 1027-1030.
[25] Guo, X.; Facchetti, A.; Marks, T. J. Imide- and Amide-Functionalized Polymer Semiconductors. *Chem. Rev.* **2014**, *114* (18), 8943-9021.
[26] Zhao, W. C.; Qian, D. P.; Zhang, S. Q.; Li, S. S.; Inganäs, O.; Gao, F.; Hou, J. H. Fullerene-Free Polymer Solar Cells with over 11% Efficiency and Excellent Thermal Stability. *Adv. Mater.* **2016**, *28* (23), 4734-4739.
[27] Zhao, J.; Li, Y.; Yang, G.; Jiang, K.; Lin, H.; Ade, H.; Ma, W.; Yan, H. Efficient organic solar cells processed from hydrocarbon solvents. *Nat. Energy* **2016**, *1*, 15027.
[28] Osedach, T. P.; Andrew, T. L.; Bulovic, V. Effect of synthetic accessibility on the commercial viability of organic photovoltaics. *Energy Environ. Sci.* **2013**, *6*, 711-718.
[29] Po, R.; Bianchi, G.; Carbonera, C.; Pellegrino, A. "All That Glisters Is Not Gold": An Analysis of the Synthetic Complexity of Efficient Polymer Donors for Polymer Solar Cells. *Macromolecules* **2015**, *48* (3), 453-461.
[30] Pirotte, G.; Kesters, J.; Verstappen, P.; Govaerts, S.; Manca, J.; Lutsen, L.; Vanderzande, D.; Maes, W. Continuous Flow Polymer Synthesis toward Reproducible Large-Scale Production for Efficient Bulk Heterojunction Organic Solar Cells. *ChemSusChem* **2015**, *8* (19), 3228-3233.
[31] Yao, Y.; Hou, J.; Xu, Z.; Li, G.; Yang, Y. Effects of Solvent Mixtures on the Nanoscale Phase Separation in Polymer Solar Cells. *Adv. Funct. Mater.* **2008**, 1*8* (12), 1783-1789.
[32] Rogers, J. T.; Schmidt, K.; Toney, M. F.; Kramer, E. J.; Bazan, G. C. Structural Order in Bulk Heterojunction Films Prepared with Solvent Additives. *Adv. Mater.* **2011**, *23* (20), 2284-2288.
[33] Galagan, Y.; de Vries, I. G.; Langen, A. P.; Andriessen, R.; Verhees, W. J. H.; Veenstra, S. C.; Kroon, J. M. Technology development for roll-to-roll production of organic photovoltaics. *Chem. Eng. Process* **2011**, *50* (5-6), 454-461.
[34] Tait, J. G.; Merckx, T.; Li, W.; Wong, C.; Gehlhaar, R.; Cheyns, D.; Turbiez, M.; Heremans, P. Determination of Solvent Systems for Blade Coating Thin Film Photovoltaics. *Adv. Funct. Mater.* **2015**, *25* (22), 3393-3398.
[35] Zhang, S.; Ye, L.; Zhang, H.; Hou, J. Green-solvent-processable organic solar cells. *Mater. Today* **2016**, *19* (9), 533-543.
[36] Aïch, B. R.; Beaupré, S.; Leclerc, M.; Tao, Y. Highly efficient thieno[3,4-c]pyrrole-4,6-dione-based solar cells processed from non-chlorinated solvent. *Org. Electron*. **2014**, *15* (2), 543-548.
[37] Sprau, C.; Buss, F.; Wagner, M.; Landerer, D.; Koppitz, M.; Schulz, A.; Bahro, D.; Schabel, W.; Scharfer, P.; Colsmann, A. Highly efficient polymer solar cells cast from non-halogenated xylene/anisaldehyde solution. *Energy Environ. Sci.* **2015**, *8*, 2744-2752.
[38] Zhang, H.; Yao, H.; Zhao, W.; Ye, L.; Hou, J. High-Efficiency Polymer Solar Cells Enabled by Environment-Friendly Single-Solvent Processing. *Adv. Energy Mater.* **2016**, *6* (6), 1502177.
[39] Heo, H.; Kim, H.; Lee, D.; Jang, S.; Ban, L.; Jim, B.; Lee, J.; Lee, Y. Regioregular D1-A-D2-A Terpolymer with Controlled Thieno[3,4-*b*]thiophene Orientation for High-Efficiency Polymer Solar Cells Processed with Nonhalogenated Solvents. *Macromolecules* **2016**, *49* (9), 3328-3335.
[40] Zhang, Z.; Zhang, X.; Zhang, J.; Gong, X.; Liu, Y.; Lu, H.; Li, C.; Bo, Z. Efficient polymer solar cells processed by environmentally friendly halogen-free solvents. *RSC Adv.* **2016**, *6*, 39074-39079.

[41] Guérette, M.; Najari, A.; Maltais, J.; Pouliot, J.-R.; Dufresne, S.; Simoneau, M.; Besner, S.; Charest, P.; Leclerc, M. New Processable Phenanthridinone-Based Polymers for Organic Solar Cell Applications. *Adv. Energy Mater.* **2016**, *6* (9), 1502094.
[42] Seri, M.; Gedefaw, D.; Prosa, M.; Tessarolo, M.; Bolognesi, M.; Muccini, M.; Andersson, M. R. A new quinoxaline and isoindigo based polymer as donor material for solar cells: Role of ecofriendly processing solvents on the device efficiency and stability. *J. Polym. Sci. A Polym. Chem.* **2016**, *55* (2), 234-242.
[43] Vanormelingen, W.; Kesters, J.; Verstappen, P.; Drijkoningen, J.; Kudrjasova, J.; Koudjina, S.; Liégeois, V.; Champagne, B.; Manca, J.; Lutsen, L.; Vanderzande, D.; Maes, W. Enhanced open-circuit voltage in polymer solar cells by dithieno[3,2-*b*:2′,3′-*d*]pyrrole *N*-acylation. *J. Mater. Chem. A* **2014**, *2*, 7535-7545.
[44] Kesters, J.; Verstappen, P.; Vanormelingen, W.; Drijkoningen, J.; Vangerven, T.; Devisscher, D.; Marin, L.; Champagne, B.; Manca, J.; Lutsen, L.; Vanderzande, D.; Maes, W. *N*-Acyl-dithieno[3,2-*b*:2′,3′-*d*]pyrrole based low bandgap copolymers affording improved open-circuit voltages and efficiencies in polymer solar cells. *Sol. Energy Mater. Sol. Cells* **2015**, *136*, 70-77.
[45] Verstappen, P.; Cardinaletti, I.; Vangerven, T.; Vanormelingen, W.; Verstraeten, F.; Lutsen, L.; Vanderzande, D.; Manca, J.; Maes, W. Impact of structure and homo-coupling of the central donor unit of small molecule organic semiconductors on solar cell performance. *RSC Adv.* **2016**, *6* (38), 32298-32307.
[46] Ahmed, E.; Subramaniyan, S.; Kim, F. S.; Xin, H.; Jenekhe, S. A. Benzobisthiazole-Based Donor–Acceptor Copolymer Semiconductors for Photovoltaic Cells and Highly Stable Field-Effect Transistors. *Macromolecules* **2011**, *44* (18), 7207-7219.
[47] Evenson, S. J.; Rasmussen, S. C. *N*-Acyldithieno[3,2-*b*:2′,3′-*d*]pyrroles: Second Generation Dithieno[3,2-*b*:2′,3′-*d*]pyrrole Building Blocks with Stabilized Energy Levels. *Org. Lett.* **2010**, *12* (18), 4054-4057.
[48] Li, W.; Yang, L.; Tumbleston, J. R.; Yan, L.; Ade, H.; You, W. Controlling Molecular Weight of a High Efficiency Donor-Acceptor Conjugated Polymer and Understanding Its Significant Impact on Photovoltaic Properties. *Adv. Mater.* **2014**, *26* (26), 4456-4462.
[49] Spoltore, D.; Vangerven, T.; Verstappen, P.; Piersimoni, F.; Bertho, S.; Vandewal, K.; Van den Brande, N.; Defour, M.; Van Mele, B.; De Sio, A.; Parisi, J.; Lutsen, L.; Vanderzande, D.; Maes, W.; Manca, J. Effect of molecular weight on morphology and photovoltaic properties in P3HT:PCBM solar cells. *Org. Electron.* **2015**, *21*, 160-170.
[50] Vangerven, T.; Verstappen, P.; Drijkoningen, J.; Dierckx, W.; Himmelberger, S.; Salleo, A.; Vanderzande, D.; Maes, W.; Manca, J. Molar Mass versus Polymer Solar Cell Performance: Highlighting the Role of Homocouplings. *Chem. Mater.* **2015**, *27* (10), 3726-3732.
[51] Katsouras, A.; Gasparini, N.; Koulogiannis, C.; Spanos, M.; Ameri, T.; Brabec, C. J.; Chochos, C. L.; Avgeropoulos, A. Systematic Analysis of Polymer Molecular Weight Influence on the Organic Photovoltaic Performance. *Macromol. Rapid Commun.* **2015**, *36* (20), 1778-1797.
[52] Hendriks, K. H.; Li, W.; Wienk, M. M.; Janssen, R. A. J. Small-Bandgap Semiconducting Polymers with High Near-Infrared Photoresponse. *J. Am. Chem. Soc.* **2014**, *136* (34), 12130-12136.
[53] Vangerven, T.; Verstappen, P.; Patil, N.; D'Haen, J.; Cardinaletti, I.; Benduhn, J.; Van den Brande, N.; Defour, M.; Lemaur, V.; Beljonne, D.; Lazzaroni, R.; Champagne, B.; Vandewal, K.; Andreasen, J. W.; Adriaensens, P.; Breiby, D. B.; Van Mele, B.; Vanderzande, D.; Maes, W.; Manca, J. Elucidating Batch-to-batch Variation Caused by Homocoupled Side Products in Solution Processable Organic Solar Cells. *Chem. Mater.* **2016**, *28* (24), 9088-9098.

[54] Lu, L.; Zheng, T.; Xu, T.; Zhao, D.; Yu, L. Mechanistic Studies of Effect of Dispersity on the Photovoltaic Performance of PTB7 Polymer Solar Cells. *Chem. Mater.* **2015**, *27* (2), 537–543.
[55] Brouwer, F.; Alma, J.; Valkenier, H.; Voortman, T. P.; Hillebrand, J.; Chiechi, R. C.; Hummelen, J. C. Using bis(pinacolato)diboron to improve the quality of regioregular conjugated co-polymers. *J. Mater. Chem.* **2011**, *21*, 1582–1592.
[56] Ghoos, T.; Van den Brande, N.; Defour, M.; Brassinne, J.; Fustin, C.-A.; Gohy, J.-F.; Hoeppener, S.; Schubert, U. S.; Vanormelingen, W.; Lutsen, L.; Vanderzande, D. J.; Van Mele, B.; Maes, W. Amphiphilic *N*-methylimidazole-functionalized diblock copolythiophenes for organic photovoltaics. *Eur. Polym. J.* **2014**, *53*, 206-214.
[57] Kesters, J.; Verstappen, P.; Raymakers, J.; Vanormelingen, W.; Drijkoningen, J.; D'Haen, J.; Manca, J.; Lutsen, L.; Vanderzande, D.; Maes, W. Enhanced Organic Solar Cell Stability by Polymer (PCPDTBT) Side Chain Functionalization. *Chem. Mater.* **2015**, *27* (4), 1332-1341.
[58] Cardinaletti, I.; Kesters, J.; Bertho, S.; Conings, B.; Piersimoni, F.; D'Haen, J.; Lutsen, L.; Nesladek, M.; Van Mele, B.; Van Assche, G.; Vandewal, K.; Salleo, A.; Vanderzande, D.; Maes, W.; Manca, J. V. Toward bulk heterojunction organic solar cells with stable active layer morphology. *J. Photon. Energy* **2014**, *4*, 040997-1–040997-12.
[59] Vandenbergh, J.; Conings, B.; Bertho, S.; Kesters, J.; Spoltore, D.; Esiner, S.; Zhao, J.; Van Assche, G.; Wienk, M. M.; Maes, W.; Lutsen, L.; Van Mele, B.; Janssen, R. A. J.; Manca, J.; Vanderzande, D. J. M. Thermal Stability of Poly[2-methoxy-5-(2'-phenylethoxy)-1,4-phenylene vinylene] (MPE-PPV):Fullerene Bulk Heterojunction Solar Cells. *Macromolecules* **2011**, *44* (21), 8470-8478.
[60] Drijkoningen, J.; Kesters, J.; Vangerven, T.; Lutsen, L.; Vanderzande, D.; Maes, W.; D'Haen, J.; Manca, J. Investigating the role of efficiency enhancing interlayers for bulk heterojunction solar cells by scanning probe microscopy. *Org. Electron.* **2014**, *15* (6), 1282-1289.
[61] Vezie, M. S.; Few, S.; Meager, I.; Pieridou, G.; Dörling, B.; Ashraf, R. S.; Goñi, A. R.; Bronstein, H.; McCulloch, I.; Hayes, S. C.; Campoy-Quiles, M.; Nelson, J. Exploring the origin of high optical absorption in conjugated polymers. *Nat. Mater.* **2016**, *15* (7), 746-753.
[62] Niklas J.; Mardis, K. L.; Banks, B. P.; Grooms, G. M.; Sperlich, A.; Dyakonov, V.; Beaupré, S.; Leclerc, M.; Xu, T.; Yu, L.; Poluektov, O. G. Highly-efficient charge separation and polaron delocalization in polymer-fullerene bulk-heterojunctions: a comparative multi-frequency EPR & DFT study. *Phys. Chem. Chem. Phys.* **2013**, *15* (24), 9562-9574.
[63] Zhou, X.; Yang, D.; Ma, D. Extremely Low Dark Current, High Responsivity, All-Polymer Photodetectors with Spectral Response from 300 nm to 1000 nm. *Adv. Optical Mater.* **2015**, *3* (11), 1570-1576.
[64] Burke, D. J.; Lipomi, D. J. Green Chemistry for organic solar cells. *Energy Environ. Sci.* **2013***, 6,* 2053-2066.